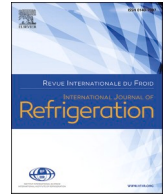




Contents lists available at ScienceDirect

International Journal of Refrigeration

journal homepage: www.elsevier.com/locate/ijrefrig

Experimental investigation of the effects of compressor types on the performance of an automobile air conditioning system using R1234yf

Étude expérimentale de l'impact des différents types de compresseurs sur les performances d'un système de conditionnement d'air automobile fonctionnant au R1234yf

Alpaslan Alkan^{a,*}, Mehmet Sait İnan^b^a Dept. of Mech. Eng., Sakarya University of Applied Sciences, 54187 Sakarya, Turkey^b Graduate Education Institute, Sakarya University of Applied Sciences, 54187 Sakarya, Turkey

ARTICLE INFO

Keywords:

Compressor
Automobile
Air conditioning
R1234yf
Exergy
Variable capacity

Mots clés:

Puissance variable
Compresseur
Conditionnement d'air
R1234yf
Exergie
Automobile

ABSTRACT

In this study, the performance of R1234yf as an alternative to R134a has been experimentally investigated in an experimental automobile air conditioning (AAC) system with variable (VCC) and fixed (FCC) capacity compressors. The AAC system was equipped with original components and instruments for mechanical measurements. The experiments were conducted for both types of compressors and refrigerants at various compressor speeds, air temperatures entering the evaporator and condenser and air speeds passing over them. The performance parameters of the AAC system have been evaluated by performing energy and exergy analysis based on the experimental data, and the results were presented in the form of comparative graphics. The experimental results show that the VCC compressor limits the refrigerant flow rate when the capacity control system is activated due to the decrease in the evaporator and condenser air inlet temperatures and the increase in the compressor speed. It was found that the coefficients of performance (COPs) of the R1234yf AAC system with VCC and FCC were approximately 13.6% and 20.1% lower than those of the R134a system with VCC and FCC, respectively. For both refrigerants, in the AAC system with VCC, the total exergy destruction rate per unit cooling capacity was 18.2% – 47.5% lower compared to the system with FCC. The R1234yf AAC system experiences lower exergy destruction in the evaporator and condenser compared to the R134a system, while it practices higher exergy destruction in the compressor and expansion device in comparison to the R134a system

1. Introduction

The development of automobile air conditioning (AAC) systems started with the discovery of chlorofluorocarbon (CFC) refrigerants in the 1930s. However, due to their harmful effects on the Ozone layer, the use of CFCs was restricted and gradually banned. R134a, a hydrofluorocarbon (HFC) refrigerant, became an alternative to CFCs in AAC systems. International agreements such as the Montreal Protocol (UNEP, 1987) and the Kyoto Protocol (GCRP, 1997) aimed to restrict and phase out the use of refrigerants which cause damage to the Ozone layer and have a high global warming potential (GWP). The European Union (Cattelan et al., 2022) has adopted legislation to restrict the use of HFCs with a GWP above 150. Research is now focusing on alternative refrigerants such as carbon dioxide (CO₂) and hydrofluoroolefins (HFOs)

such as R1234yf.

The compressor is an important component of vapour compression refrigeration (VCR) cycles. They compress the refrigerant from superheated low-pressure vapour to superheated high-pressure vapour. Two different types of compressors, fixed and variable capacity compressors (FCC and VCC), are commonly used in the AAC system. In the AAC system with an FCC, the refrigerant flow rate is a function of the engine speed driving the compressor, while in the system with a VCC, the refrigerant flow rate does not depend on the engine speed, but it is controlled by the capacity control system to keep the suction pressure above a predetermined value (Daly, 2006).

The literature studies on the AAC system generally dealt with the comparison of the performance parameters for different refrigerants and system components based on experimental and theoretical applications. Zilio et al. (2011) found that the cooling capacity and coefficient of

* Corresponding author.

E-mail address: aalkan@subu.edu.tr (A. Alkan).<https://doi.org/10.1016/j.ijrefrig.2023.09.004>

Received 21 March 2023; Received in revised form 4 September 2023; Accepted 5 September 2023

Available online 7 September 2023

0140-7007/© 2023 Elsevier Ltd and IIR. All rights reserved.

Nomenclature

AAC	Automotive air conditioning
c_p	Specific heat, $\text{kJ kg}^{-1} \text{K}^{-1}$
CFC	Chlorofluorocarbon
COP	Coefficient of performance
$\dot{E}x_d$	Rate of exergy destruction, kW
FCC	Fixed capacity compressor
GWP	Global warming potential
K	Temperature, Kelvin
h	Specific enthalpy, kJ kg^{-1}
HFC	Hydrofluorocarbon
HFO	Hydrofluoroolefin
IHX	Internal heat exchanger
\dot{m}	Mass flow rate, kg s^{-1}
ODP	Ozone depleting potential Pressure, kPa
OT	Orifice tube
\dot{Q}	Heat transfer rate, kW
R	Ideal gas constant, $\text{kJ kg}^{-1} \text{K}^{-1}$
s	Specific entropy, $\text{kJ kg}^{-1} \text{K}^{-1}$
T	Temperature, K or $^{\circ}\text{C}$
T_0	Dead state temperature, K

TXV	Thermostatic expansion valve
VCC	Variable capacity compressor
VCR	Vapour compression refrigeration
\dot{W}	Power, kW

Greek symbols

ω	Humidity ratio
ψ	Specific flow exergy, kJ kg^{-1}

Subscripts

0	Dead state
an	Air
ai	Air inlet
$comp$	Compressor
$cond$	Condenser
cv	Control volume
$evap$	Evaporator
in	Inlet
out	Outlet
r	Refrigerant
tot	Total
v	Water vapour

performance (COP) of the R1234yf system were significantly lower than those of the R134a one. However, the performance values of R1234yf could approach those of R134a by adjusting the thermostatic expansion valve (TXV) and optimizing the VCC control valve. Lee and Jung (2012) experimentally evaluated the performance of R134a and R1234yf in an AAC system. According to their results, R1234yf caused 0.8–2.7% lower COP, up to 4.0% lower cooling capacity and 6.4 $^{\circ}\text{C}$ –6.7 $^{\circ}\text{C}$ lower compressor discharge temperature in comparison to R134a. Navarro-Esbri et al. (2013) investigated the experimental performance of a VCR system using R1234yf and reported a 19% lower COP and a 9% lower cooling capacity compared to R134a. Navarro et al. (2013) tested R1234yf, R134a and R290 in a bus air conditioning system. They concluded that the compressor discharge temperature of R1234yf was about 10 K lower than the compressor discharge temperature of R290 and R134a. Mota-Babiloni et al. (2014) investigated the effects of R1234yf, R1234ze(E) and R134a on the performance of an air conditioning system with an open reciprocating compressor. They found that R1234yf and R1234ze(E) caused about 9% and 30% lower cooling capacity than R134a, respectively, and R1234yf and R1234ze(E) yielded 7% and 6% lower COP than R134a, respectively. Yatanbaba et al. (2015) studied the theoretical exergy analysis of a VCR system with two evaporators for R1234yf and R1234ze(E) as alternatives to R134a. They found that, although the values of the performance parameters of the system with R1234yf are lower than those with R134a, the difference is small, and therefore, it can be a good alternative to R134a due to its environmentally friendly properties. Furthermore, they showed that R1234ze(E) could replace the conventional R134a after a minor design change, as its performance parameters were almost similar. Daviran et al. (2017) compared the performance parameters of an AAC system with R134a and R1234yf for a continuous mass flow rate and cooling capacity by using a simulation developed in MATLAB. They demonstrated that the COP of the R1234yf system was 1.3–5% lower than that of the R134a one at fixed refrigeration capacity and 18% higher than that of R134a at a fixed refrigerant mass flow rate. Golzari et al. (2017) studied the performance analysis of an AAC system with R134a and R1234yf using a computer program. They showed that the use of R1234yf resulted in higher exergy efficiency in comparison to the use of R134a and that the compressor was the component where maximum entropy generation and maximum exergy destruction occurred. Gaurav and Kumar (2018) conducted a simulation study to investigate the

performance and exergy levels of AAC systems. In the study, a steady-state operation was assumed and kinetic and potential energy and exergy losses in all components as well as pressure losses in the piping were neglected. They found that R1234yf caused the highest refrigerant mass flow rate, followed by R134a and R1234ze(E), respectively. However, R134a yielded the highest COP values, followed by R1234yf and R1234ze(E), respectively. Aral et al. (2021) conducted experiments on an AAC system with heat pump feature using R134a and R1234yf under a wide range of compressor speeds and air inlet temperatures for cooling and heating modes. Their experimental results showed that, on average, the R1234yf system had 5.8% less cooling capacity, 0.2% more heating capacity, 11.9% less COP for cooling and 3.6% less COP for heating compared to R134a. Alkan et al. (2021) investigated the experimental performance of an AAC system with an FCC compressor using R134a and R1234yf refrigerants for different compressor speeds as well as condenser and evaporator air inlet temperatures. They found that R1234yf had a 0.4–10.9% lower cooling capacity, a 5.5–11.6% lower COP and a 4.7–16.1 $^{\circ}\text{C}$ lower compressor discharge temperature compared to R134a. Tasdemirci et al. (2022) set up an AAC with a VCC and conducted comparative energy and exergy analyses of the system for R1234yf and R134a by varying the test conditions over a wide range. They found that, on average, the R1234yf system had a 13.7% lower cooling capacity than the R134a one and had a 12.8% lower COP based on total power consumption. They concluded that the system with R1234yf destroyed an average of 18.9% more exergy per unit cooling capacity. Khatoun and Karimi (2023) conducted a theoretical analysis of a VCR system with two evaporators. They investigated the energy and exergy performance of the system for different condenser and evaporator temperatures. They determined the performance of low GWP refrigerants such as R1234yf, HFO1336mzz (Z), R513A and R450A in comparison to some high GWP refrigerants, namely R134a and R452A. Their results showed that the maximum exergy efficiency and COP as well as the lowest compressor power were obtained with HFO1336mzz(Z), which were 31.50%, 2.47 and 6.304 kW, respectively.

Alkan and Hosoz (2010a) developed an experimental R134a AAC system with the ability to operate using FCC and VCC. They tested the system under steady-state operating conditions for each compressor by varying the compressor speed, the temperatures of the air streams entering the condenser and evaporator, and the speeds of these air

streams. They found that the system with VCC provided a higher COP than the one with FCC, although it yielded a lower cooling capacity. They also determined that the cooling capacity and total exergy destruction in the system with VCC remained almost constant over a certain compressor speed, while both parameters increased continuously with the compressor speed in the system with FCC. Alkan and Hosoz (2010b) experimentally investigated the effects of two different types of expansion devices, namely an orifice tube (OT) and a TXV, on the performance values in an R134a AAC system with a VCC. Using the performance values obtained with both expansion devices, they determined that the cooling capacity generally increases with the compressor speed. However, COP decreased and the exergy destruction in the system increased with rising compressor speed. In addition, the use of TXV generally resulted in slightly higher cooling capacity and COP, but lower exergy destruction compared to the use of OT. Cho and Park (2016) experimentally investigated the effect of employing an internal heat exchanger (IHX) on the performance of an AAC. They suggested that the optimal charge for the system with R1234yf should be 10% lower than that for the system with R134a. Their experiments showed that the COP and the cooling capacity of the system with R1234yf were 3.6–4.5% and 4.0–7.0% lower than that with R134a, respectively. Furthermore, the use of IHX caused the performance of the R1234yf system to approach that of the R134a one. Mendoza-Miranda et al. (2016) evaluated the performance of R1234yf, R1234ze(E) and R450A as alternatives to R134a in a refrigeration system with a variable speed compressor. The Buckingham p-theorem was used to build a compressor model based on dimensionless numbers supported by experimental data. The prediction error of the model was 10% and less than 2 K for temperature. According to the results of this study, the COP values of the system with R1234yf, R450A and R1234ze(E) were lower than that with R134a. Devocioğlu and Oruç (2018) experimentally investigated the performance of R1234ze(E) and R1234yf as alternatives to R134a in a refrigeration system with an FCC. They employed a plate-type IHX instead of a concentric tube-type IHX, which was used in previous studies. They found that the use of IHX increased both the refrigerant charge and COP for all cases, with the lowest COP for R1234yf, then R1234ze(E) and the highest one for R134a. Wantha (2019) experimentally and theoretically investigated the heat transfer characteristics of R134a and R1234yf in a VCR system with a tube-type IHX. Their results showed that the use of IHX increased the COP of the R1234yf system by 3.78% and the COP of the R134a one by 2.11%. Li et al. (2022) simulated a VCR system with a VCC in MATLAB/Simulink. They found that the modelling results differed by $\pm 10\%$ from the experimental data. They showed that the VCR system with a VCC can provide high-efficiency capacity control for various conditions. They found that the system could achieve 144 W cooling capacity with a COP of 2.75 at a 14 mm compressor stroke and 5 °C evaporating temperature, while it achieved a 17 W cooling capacity with a COP of 2.2 at a 10 mm compressor stroke.

It is seen that most of the experimental studies in the literature were performed under a limited range of test conditions, while some studies were entirely theoretical. Furthermore, the common compressor type used in these studies was FCC and there were very few studies on the performance of AAC systems with R1234yf employing a VCC. In this study, an AAC system with VCC and FCC compressors was set up in a laboratory environment, and the experiments were conducted with R134a and its substitute R1234yf at different compressor speeds, condenser and evaporator air inlet temperatures and air speeds. Although the conditioned air temperature was studied as a function of time, other performance parameters of the system were obtained based on steady-state data, which were obtained by applying energy and exergy analysis to the system. The considered performance parameters were the air temperature at the evaporator outlet, refrigerant mass flow rate, cooling capacity, compressor power, COP, compressor discharge temperature, exergy destruction rate in the components, and total exergy destruction rate per unit cooling capacity for both refrigerant cases and compressor types.

2. Description of the test setup

The schematic diagram of the experimental AAC system is shown in Fig. 1. The components of the refrigeration cycle of the experimental system are a seven-cylinder VCC and a seven-cylinder FCC, a micro-channel condenser, a liquid tank, a filter/dryer, a TXV, and a laminated-type evaporator. The components employed in the system along with their specifications are listed in Table 1.

The experimental setup was designed to simulate realistic climatic conditions. It has 1 m long air ducts containing the evaporator and condenser along with a centrifugal fan placed at the inlet of the evaporator duct and axial fans placed at the outlet of the condenser duct. In these ducts, a heating resistance with a power of 5.4 kW is located upstream of the condenser and another resistance with a power of 1.8 kW is located upstream of the evaporator. An electric motor with a power of 5.5 kW drives both compressors of the experimental system through a belt-pulley mechanism. The electric motor is controlled by a frequency inverter to achieve the desired compressor speed.

The experimental AAC system is equipped with various measuring instruments to perform a comparative performance analysis and to control the operation of the system. The temperature and pressure data of the refrigerant circulating in the AAC system are taken at the points with the symbols T and P, respectively, as shown in Fig. 1. The refrigerant temperature data were obtained using T-type thermocouples, while pressure data were obtained using pressure transmitters. The refrigerant mass flow rate was measured by a Coriolis mass flow sensor placed in the liquid line. The temperature (T), relative humidity (RH) and velocity (V_a) of the air streams in the experimental system were measured at the points shown in Fig. 1. The temperature and relative humidity were measured using an SHT 71 temperature and humidity sensor. The velocities of the air streams flowing over the evaporator and condenser were measured with air flow meters located at the points where the average velocity values were obtained. The compressor speed was measured using an inductive proximity sensor. The characteristics of the measuring devices used in the experimental system are listed in Table 2.

The data received from the sensors in the experimental system were acquired and transmitted to the computer using the RS485 MODBUS communication protocol. The data transmitted to the computer were recorded during a certain experimental period, and at the same time, a data flow was established to the control devices that met the desired experimental conditions in the experimental system. Experimental comparisons were made as a function of compressor speed, evaporator, and condenser air inlet temperatures and speeds. The compressor speed as well as the condenser and evaporator air inlet temperatures were controlled by a PLC circuit and set to the desired values. The desired air speeds in the evaporator and condenser ducts were provided by the evaporator and condenser fans controlled by DC motor drives. The compressors were connected to the refrigeration circuit through hand valves, as shown in Fig. 1. The desired compressor was activated by opening its valves and switching on its electromagnetic clutch, while the valves of the passive compressor were closed. The photographs of the experimental AAC system along with its compressor connections are shown in Fig. 2. More detailed information about the experimental system can be found in Inan (2021).

3. Testing procedure

The experimental performance of the AAC system with R134a and R1234yf was investigated for VCC and FCC. Various properties of the refrigerants are listed in Table 3. In the experiments with R134a, 2500 g of R134a was charged into the AAC system, while in the experiments with R1234yf, 2250 g of refrigerant was charged. Following Cho et al. (2013), the charge of R1234yf is 250 g less than that of R134a since the liquid density of R1234yf is 10% lower than that of R134a. First, the tests with R134a were conducted as baseline tests, and then, those with

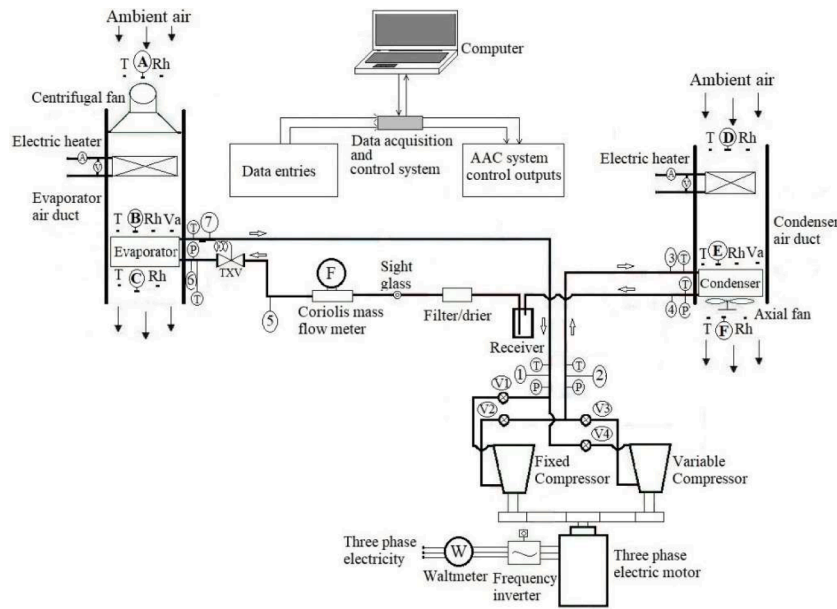


Fig. 1. Schematic representation of AAC system with different compressor types.

Table 1
Technical specifications of the components.

Component	Specifications
Compressors	Type: 7-cylinder, wobble-plate, FCC, Stroke volume: 154.9 cc rev ⁻¹ Type: 7-cylinder, wobble-plate, VCC, Stroke volume: 161.3 cc rev ⁻¹
Condenser	Type: Parallel flow, micro-channel Size: 0.63 m × 0.380 m × 0.020 m
Evaporator	Type: Laminated Size: 0.235 m × 0.220 m × 0.065 m
Expansion device	Type: Internally equalized thermostatic expansion valve Capacity: 5.5 kW

Table 2
Characteristics of the measuring instruments.

Physical variable	Apparatus	Range	Uncertainty
Temperature (Refrigerant)	Thermocouple (Type T)	−40/350 °C	±0.5 °C
Air dry-bulb temperature	SHT 71	−40/123 °C	±0.4 °C
Pressure	Transmitter (Vika S–10)	0/25 bar	0.25 bar
Relative humidity	SHT 71	0/100%	±3%
Air velocity	Transmitter (EE65–VCK200)	0.2/10 m s ⁻¹	±0.2 m s ⁻¹
Mass flow rate	Coriolis flow meter (Krohne Optimass 3300C H04)	0/450 kg h ⁻¹	±0.1%

R1234yf were performed. The tests were conducted as transient and steady-state ones. The compressor speed was adjusted to 750 rpm and 2250 rpm, while the evaporator and condenser air speeds were set to 3 m s⁻¹ and 3.4 m s⁻¹, respectively, and the air inlet temperatures of the condenser and evaporator were set as T_{cond, ai} = 35 °C and T_{evap, ai} = 40 °C, respectively, for the transient tests. On the other hand, the steady-state tests were performed at T_{cond, ai} = T_{evap, ai} = 25 °C and T_{cond, ai} = T_{evap, ai} = 40 °C and the compressor speeds were adjusted to 750, 1150, 1450 and 1750 rpm in the tests conducted at the evaporator and condenser air inlet temperatures of 25 °C. On the other hand, the compressor speed was adjusted to 750, 1250, 1750, 2250 and 2750 rpm in the tests conducted at the evaporator and condenser air inlet temperatures of 40 °C. In the steady-state tests, the evaporator and

condenser air speeds were set to 2 m s⁻¹ and 3.4 m s⁻¹, respectively. In addition, in the T_{evap, ai} = 40 °C and T_{evap, ai} = 25 °C air inlet temperature tests, the relative humidity of the air stream entering the evaporator was maintained at 30±2% and 65±5% for all systems, respectively. Before starting a test, the inputs of the desired condenser and evaporator air inlet temperatures, air speeds and compressor speed were entered through the user interface of the experimental system, and the control system operated the system to achieve the desired input conditions. The steady-state performance of the system was evaluated using the steady-state data, which were usually collected between the tenth and fifteenth minutes of the operation after reaching stabilized pressures and temperatures.

4. Thermodynamic analysis

The first law of thermodynamics can be applied to the AAC system to evaluate its energetic performance parameters. In the thermodynamic analysis, it is assumed that the kinetic and potential energy variations are negligible, and there is no pressure drop in the condenser, evaporator, and refrigerant lines. In this study, the values of entropy and enthalpy were determined using the REFPROP 9.1 software (Lemmon et al., 2018).

In the AAC system, the cooling capacities for each case can be evaluated using the enthalpy and mass flow rates of the refrigerants at the inlet and outlet of the evaporator with the following equation

$$\dot{Q}_{evap} = \dot{m}_r (h_7 - h_6) \quad (1)$$

Assuming that the compressors used in the AAC system are adiabatic, the compression work delivered to the refrigerants in the compressors can be determined from

$$\dot{W}_{comp} = \dot{m}_r (h_2 - h_1) \quad (2)$$

The COP for the vapour compression refrigeration cycle can be determined from the ratio of refrigeration capacity to compressor power.

$$COP = \frac{\dot{Q}_{evap}}{\dot{W}_{comp}} \quad (3)$$

The second law of thermodynamics can be used to determine the thermodynamic inefficiency of the components in the AAC system. The

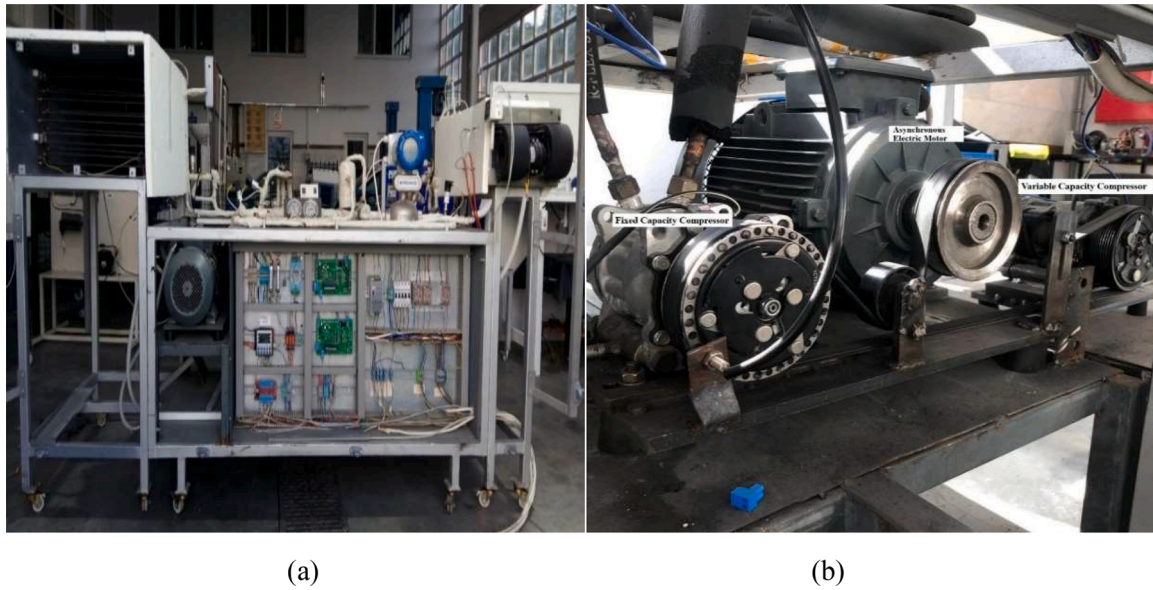


Fig. 2. Pictures of the experimental system; (a) General view, (b) Connection between the compressors and electric motor.

Table 3
Characteristics of refrigerants (Mota-Babiloni et al., 2014; Lemmon et al., 2018).

Refrigerant	R134a	R1234yf
Chemical formula	C ₂ H ₂ F ₄	C ₃ H ₂ F ₄
Molecular weight (kg kmol ⁻¹)	102	114
Boiling point at 101.325 kPa (°C)	-26.07	-29.45
Critical temperature (°C)	101.06	94.70
Critical pressure (kPa)	4059	3382
Liquid density at 0 °C (kg m ⁻³)	1294.8	1176.3
Vapour density at 0 °C (kg m ⁻³)	14.428	17.6
Latent heat of vaporization at 0 °C (kJ kg ⁻¹)	198.60	163.29
ODP	0	0
GWP	1430	4
ASHRAE Safety Group	A1	A2L

equation for the exergy balance can be given for a given control volume as follows (Kumar et al., 2020)

$$\sum \left(1 - \frac{T_0}{T_j}\right) \dot{Q}_j + \sum \dot{m}_{in} \psi_{in} = \sum \dot{m}_{out} \psi_{out} + \dot{W}_{cv} + \dot{E}x_d \quad (4)$$

In this equation, \dot{Q}_j is the heat transfer rate at the location on the boundary, T_j is boundary temperature, \dot{W}_{cv} is the work produced in the control volume, $\dot{E}x_d$ is the exergy destroyed in the control volume and ψ is the specific flow exergy of the refrigerant defined as

$$\psi = (h - h_0) - T_0(s - s_0) \quad (5)$$

where the subscript “0” represents the state of the system in the dead state, i.e., at ambient conditions. The specific flow energies of the air at points B, C, and E shown in Fig. 1 are determined by the following equation (Hosoz et al., 2015; Ozgener and Hepbasli, 2007)

$$\begin{aligned} \psi_a = & (c_{p,a} + \omega c_{p,v}) T_0 \left[\left(\frac{T}{T_0}\right) - 1 - \ln\left(\frac{T}{T_0}\right) \right] \\ & + \left[(1 + 1.6078 \omega) R_a T_0 \ln\left(\frac{P}{P_0}\right) \right] \\ & + R_a T_0 \left\{ \left(1 + 1.6078 \omega\right) \ln\left(\frac{1 + 1.6078 \omega_0}{1 + 1.6078 \omega}\right) + 1.6078 \omega \ln\left(\frac{\omega}{\omega_0}\right) \right\} \end{aligned} \quad (6)$$

The rates of exergy destroyed in the components of the AAC system were obtained from Eq. (4) and the resulting equations were presented

in Table 4. In these equations, $\dot{m}_{a,cond}$ and $\dot{m}_{a,evap}$ denote the air mass flow rates passing over the condenser and evaporator, respectively.

The exergy destroyed in the entire AAC system can be expressed as

$$\dot{E}x_{d,tot} = \dot{E}x_{d,comp} + \dot{E}x_{d,cond} + \dot{E}x_{d,TVX} + \dot{E}x_{d,evap} \quad (7)$$

5. Uncertainty analysis

The Moffat (1988) method was used to calculate the uncertainties of the performance parameters of the AAC system. If a function y is to be studied from a range of fully n measurable variables, that is x_1, x_2, \dots, x_n , the uncertainty of the y function can be evaluated from

$$u_y = \sqrt{\sum_{i=1}^n \left(\frac{\partial y}{\partial x_i} u_{x_i}\right)^2} \quad (8)$$

where u_{x_i} indicates the uncertainty of the measured variable.

Using experimental data and the accuracy of the instruments provided in Table 2, the maximum uncertainties of the cooling capacity, compressor power and COP were found to be 0.0399 kW, 0.0409 kW and 0.0293, respectively.

6. Results and discussion

Various performance parameters of the experimental AAC system with R134a and R1234yf for FCC and VCC are shown in Figs. 3–11. The performance parameters are presented as a function of the evaporator and condenser air inlet temperatures, air speeds, and compressor speed.

The change in the conditioned air temperature leaving the evaporator as a function of time is indicated in Fig. 3. It is seen that the air temperature leaving the evaporator reaches a stable value in 2–4 min after starting up the system, depending on the compressor type and compressor speed for both refrigerants. At the compressor speed of 750

Table 4
The expressions for the exergy destroyed in the components of the AAC system.

Component	Expression
Compressor	$\dot{E}x_{d,comp} = \dot{m}_r(\psi_{comp,in} - \psi_{comp,out}) + \dot{W}_{comp}$
Condenser	$\dot{E}x_{d,cond} = \dot{m}_r(\psi_{cond,in} - \psi_{cond,out}) + \dot{m}_{a,cond}(\psi_E - \psi_F)$
Expansion valve	$\dot{E}x_{d,TVX} = \dot{m}_r(\psi_{TVX,in} - \psi_{TVX,out})$
Evaporator	$\dot{E}x_{d,evap} = \dot{m}_r(\psi_{evap,in} - \psi_{evap,out}) + \dot{m}_{a,evap}(\psi_B - \psi_C)$

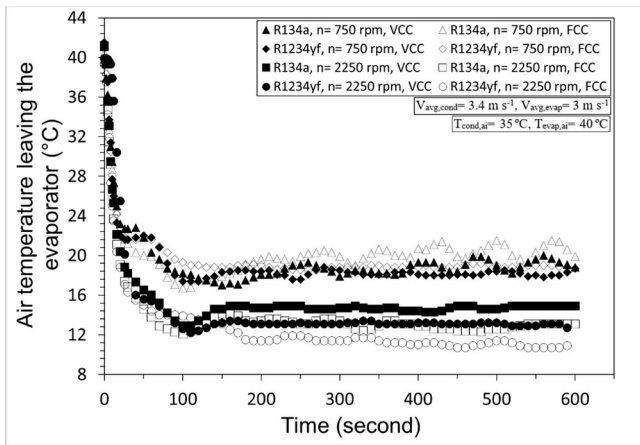


Fig. 3. The air temperature leaving the evaporator as a function of time.

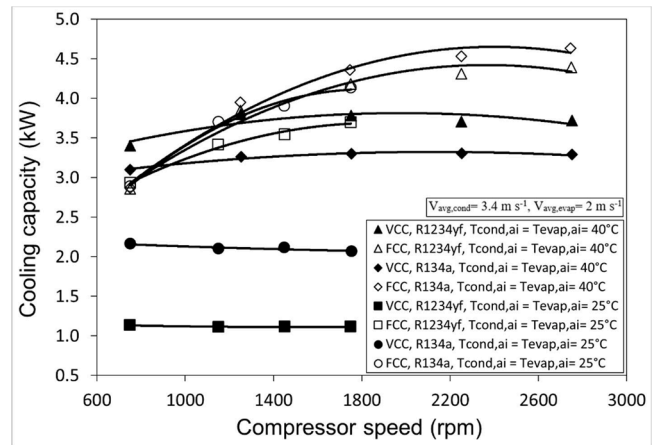


Fig. 6. The cooling capacity with respect to compressor speed.

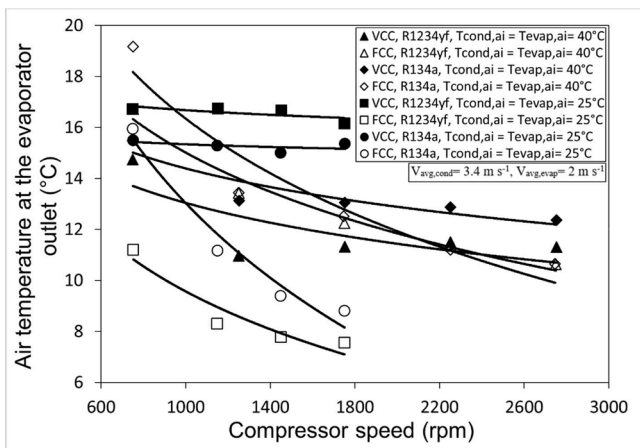


Fig. 4. The steady-state air temperature leaving the evaporator as a function of compressor speed.

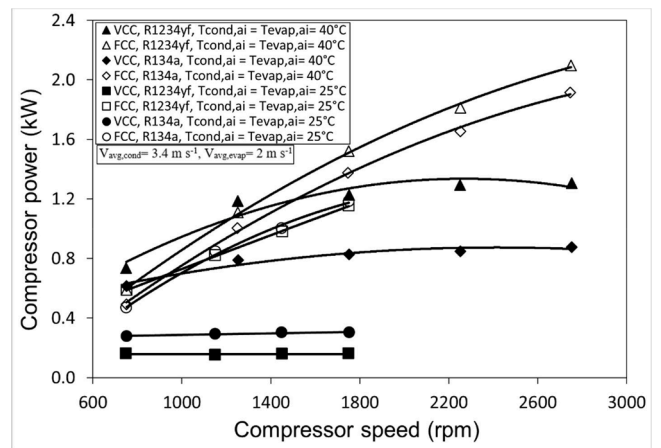


Fig. 7. The compressor power with respect to compressor speed.

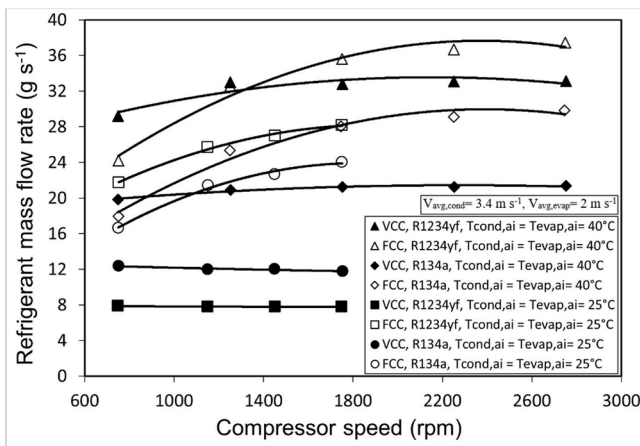


Fig. 5. The refrigerant mass flow rate with respect to the compressor speed.

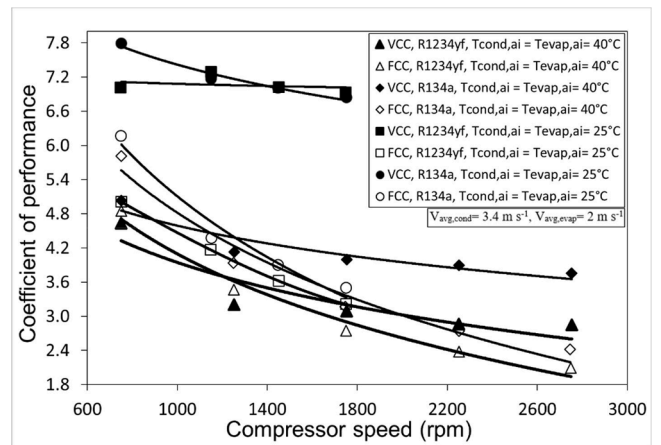


Fig. 8. The COP with respect to compressor speed.

rpm, the steady-state value of air temperature leaving the evaporator was 18.60 °C and 18.22 °C for R134a and R1234yf, respectively, when the VCC was employed. On the other hand, the air temperature leaving the evaporator stabilized at 20.14 °C and 18.95 °C for R134a and R1234yf, respectively, when the FCC was employed. In the system with R134a and at the compressor speed of 2250 rpm, the air temperature leaving the evaporator was stabilized at 14.59 °C and 13.02 °C for VCC

and FCC, respectively. In the system with R1234yf and at the compressor speed of 2250 rpm, the air temperature leaving the evaporator was stabilized at 13.13 °C and 11.68 °C for VCC and FCC, respectively.

The change in the conditioned air temperature at the evaporator outlet as a function of compressor speed is given in Fig. 4. In the case of $T_{cond, ai} = T_{evap, ai} = 40\text{ °C}$, the air temperatures at the evaporator outlet decreased by approximately 3.28 and 7.30 °C with the increase in the compressor speed from 750 rpm to 2750 rpm in the cases of VCC and

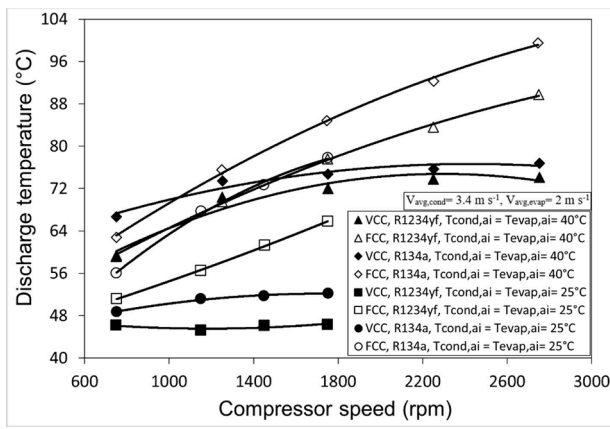


Fig. 9. The compressor discharge temperature with respect to compressor speed.

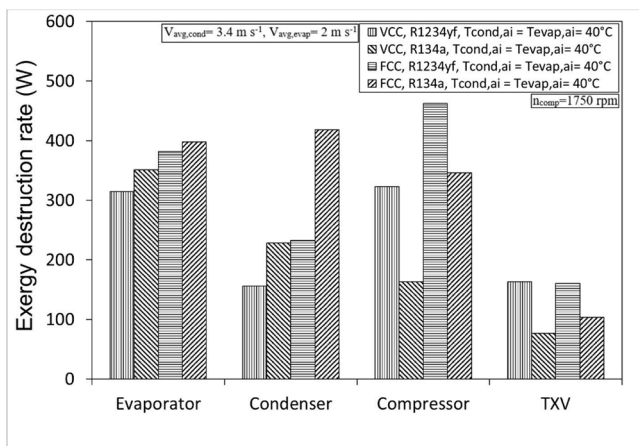


Fig. 10. The exergy destruction rate in the components with respect to compressor speed.

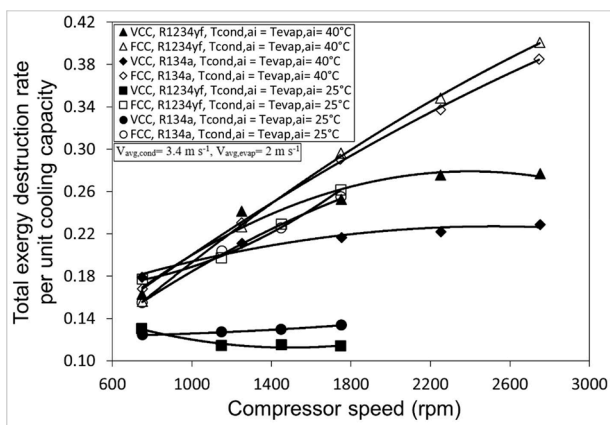


Fig. 11. The total exergy destruction rate per unit cooling capacity with respect to compressor speed.

FCC, respectively. When $T_{cond,ai} = T_{evap,ai} = 25 \text{ }^\circ\text{C}$, the air temperatures at the evaporator outlet decreased by approximately 0.36 and 5.39 °C with the increase in the compressor speed from 750 rpm to 1750 rpm in the cases of VCC and FCC, respectively. Due to the activation of the capacity control system, the conditioned air temperature did not considerably drop in the case of VCC. For R1234yf, at the condition of $T_{cond,ai} = T_{evap,ai} = 40 \text{ }^\circ\text{C}$, the evaporator air outlet temperature was

found to be on average 1.4 and 0.5 °C less for the cases of VCC and FCC, respectively, in comparison to R134a. For $T_{cond,ai} = T_{evap,ai} = 25 \text{ }^\circ\text{C}$, the R1234yf yielded on average 2.6 °C lower evaporator air outlet temperature than R134a in the system with FCC compressor, while in the system with VCC, the R1234yf caused on average 1.3 °C higher evaporator air outlet temperature. Thus, at the low evaporator and condenser inlet air temperatures, when R1234yf was used, the capacity control system of the VCC was activated earlier in comparison to the use of R134a.

The variation of the refrigerant mass flow rate in the experimental AAC system with respect to the compressor speed is presented in Fig. 5. Although the mass flow rate of the refrigerant circulating in the AAC system with the VCC remains almost constant for $T_{cond,ai} = T_{evap,ai} = 25 \text{ }^\circ\text{C}$, it slightly increases with rising compressor speed for $T_{cond,ai} = T_{evap,ai} = 40 \text{ }^\circ\text{C}$. It was observed that the mass flow rates of R1234yf and R134a increased by 13.5% and 7.7%, respectively, when the speed of the VCC was increased from 750 rpm to 2750 rpm for $T_{cond,ai} = T_{evap,ai} = 40 \text{ }^\circ\text{C}$. For the same air inlet temperatures, the mass flow rates of R1234yf and R134a increased by 54.6% and 66.3%, respectively, when the speed of the FCC compressor was increased from 750 rpm to 2750 rpm. The capacity control system of the VCC, which was activated due to the decrease in the compressor inlet pressure with rising compressor speed, reduced the displacement of the compressor, thus limiting the refrigerant mass flow rate circulating in the system with the VCC compared to the FCC. It was found that the refrigerant mass flow rates of R1234yf and R134a in the system with the VCC decreased by approximately 74.7% and 41.2%, respectively, when the condenser and evaporator air inlet temperatures were dropped from 40 °C to 25 °C. Furthermore, the mass flow rates of R1234yf and R134a in the system with FCC decreased by approximately 15.6% and 10.8%, respectively, when the condenser and evaporator air inlet temperatures were dropped from 40 °C to 25 °C. On the contrary, the mass flow rates of R1234yf and R134a in the AAC system with VCC for $T_{cond,ai} = T_{evap,ai} = 25 \text{ }^\circ\text{C}$ decreased only by 1.2% and 4.9%, respectively, when the compressor speed was increased from 750 rpm to 1750 rpm as a result of the activation of the capacity control system. However, for R1234yf and R134a, the refrigerant mass flow rate in the system with the FCC increased with the compressor speed by 29.8% and 44.5%, respectively. The mass flow rate of R1234yf is higher than that of R134a due to its higher vapour density at a certain saturation temperature. However, the capacity control system of the VCC is activated more effectively when the refrigerant is R1234yf, thus resulting in a lower refrigerant mass flow rate when the inlet air temperatures of the evaporator and condenser decrease.

The change in the cooling capacity of the AAC system as a function of compressor speed is shown in Fig. 6. Except for $T_{cond,ai} = T_{evap,ai} = 25 \text{ }^\circ\text{C}$ for the case of VCC, the cooling capacity of the system with R1234yf and R134a usually increases with rising compressor speed. The cooling capacity of the system with R1234yf and R134a increased by 9.4% and 6.2%, respectively, with rising compressor speed when the VCC was used for $T_{cond,ai} = T_{evap,ai} = 40 \text{ }^\circ\text{C}$. However, it was observed that the cooling capacity of the system with VCC using R1234yf and R134a for $T_{cond,ai} = T_{evap,ai} = 25 \text{ }^\circ\text{C}$ decreased by 2.2% and 4.3%, respectively, with the increase in compressor speed. In the AAC system with the VCC, the cooling capacities of the system with R1234yf and R134a were in the range of 1.11–3.80 kW and 2.07–3.11 kW, respectively. In the AAC system with the FCC, the cooling capacities for R1234yf and R134a were in the range of 2.86–4.39 kW and 2.88–4.63 kW, respectively.

The change in the compressor power as a function of compressor speed is shown in Fig. 7. Excepting $T_{cond,ai} = T_{evap,ai} = 25 \text{ }^\circ\text{C}$ with the VCC, the compressor power of the AAC system usually increases with rising compressor speed for both compressor cases. In the AAC system with the VCC, a compressor power of 0.15–1.30 kW and 0.28–0.88 kW was observed for R1234yf and R134a, respectively. In the AAC system with the FCC, a compressor power of 0.59–2.10 kW and 0.47–1.92 kW was obtained for R1234yf and R134a, respectively.

The variation of COP for the AAC system as a function of the compressor speed is indicated in Fig. 8. It is seen the COP generally decreases with rising compressor speed for all systems. For $T_{\text{cond,ai}} = T_{\text{evap,ai}} = 40^\circ\text{C}$, the AAC system with R1234yf using VCC and FCC had on average 13.6% and 20.1% less COP than the system with R134a using the same compressors, respectively. For $T_{\text{cond,ai}} = T_{\text{evap,ai}} = 25^\circ\text{C}$, the COP for the R1234yf system was on average 1.1% higher than the COP for the R134a one, which is because the capacity control system of the VCC system is more effective in the system with R1234yf than that with R134a at high compressor speeds. Under the same conditions, the R1234yf system with FCC yielded on average 9.8% less COP than the R134a one.

The variation of compressor discharge temperature as a function of the compressor speed with FCC and VCC is shown in Fig. 9. The compressor discharge temperature usually tends to increase with rising compressor speed for both compressors, except for $T_{\text{cond,ai}} = T_{\text{evap,ai}} = 25^\circ\text{C}$ with VCC. The capacity control system in the VCC was activated due to the increase in the compressor speed and decrease in the evaporator and condenser air inlet temperatures, which limits the increasing trend in the compressor discharge temperature. It was found that the AAC system using R1234yf with VCC and FCC has 1.87–7.51 °C and 3.44–12.03 °C lower compressor discharge temperatures, respectively, than the system with R134a for the same compressor types. The low compressor discharge temperature is usually desirable as it extends the life of the oil used in the refrigeration system, but as it reduces the heat dissipation in the condenser, a larger condenser heat transfer area is required.

The amount of exergy destroyed in the components of the AAC system is exhibited in Fig. 10 for the compressor speed of 1750 rpm. The exergy destroyed in the evaporator and condenser is caused by the temperature difference between the refrigerant and air streams passing through and over them. Since the capacity control system of the VCC is activated at rising compressor speed, the refrigerant mass flow tends to be constant. At the same time, the amount of exergy destroyed in the evaporator of the system with the VCC is less for both refrigerants than that with the FCC, which is due to the decreasing trend of air temperature leaving the evaporator. It was found that the AAC system with the VCC compressor destroyed 17.6% and 11.7% less exergy in the evaporator for R1234yf and R134a, respectively, than that with the FCC. The AAC system using R1234yf with the VCC and FCC destroyed 31.7% and 44.4% less exergy in the condenser than that using R134a for the same compressor types, respectively. This is originated from the fact that the compressor discharge temperature of the system with R1234yf is lower than that with R134a. As the compressor discharge temperature rises, the amount of exergy destroyed in the condenser increases because the difference between the temperature of the refrigerant in the condenser and the air stream passing over its surface increases. In the AAC system, the amount of exergy destroyed in the compressor increases as the mass flow rate of the refrigerant gets higher. The capacity control system of the VCC, which is activated as a function of the compressor speed, reduces the increasing tendency of the refrigerant mass flow rate compared to the FCC. The test results show that the amount of exergy destroyed in the VCC for R1234yf and R134a is 30.2% and 52.7% lower, respectively, compared to the FCC for the same refrigerants. Due to the high mass flow rate of R1234yf despite the low-pressure ratio in the compressor, the amount of exergy destroyed in the compressor was found to be 49.4% and 25.3% higher than that for R134a with VCC and FCC, respectively. As the mass flow rate of R1234yf is high, the amount of exergy destroyed in the TXV for VCC and FCC compressors is 52.9% and 35.3% higher than that obtained with R134a, respectively, for the same compressor types.

The total amount of exergy destroyed per unit cooling capacity is shown in Fig. 11. The total amount of exergy destroyed per unit cooling capacity of the AAC system usually increases with rising compressor speed, excepting the case of $T_{\text{cond,ai}} = T_{\text{evap,ai}} = 25^\circ\text{C}$ in the system with a VCC. When the VCC is used, this increasing tendency stops due to the

activation of the capacity control system at high compressor speeds. It can be observed that the total amount of exergy destroyed per unit cooling capacity decreases slightly, especially at the low condenser and evaporator air inlet temperatures, and that the capacity control system becomes more effective for R1234yf with rising compressor speed. As the compressor speed increases, the evaporator temperature decreases as a result of the decrease in the compressor suction pressure, while the condenser pressure increases as a result of the increase in the compressor discharge pressure. As a result, the temperature difference between the refrigerant and air stream temperatures in the heat exchangers of the AAC system rises together with the increase in the pressure difference across the compressor and TXV. Furthermore, excepting the case of $T_{\text{cond,ai}} = T_{\text{evap,ai}} = 25^\circ\text{C}$ in the system with VCC, the refrigerant mass flow rate increases with rising compressor speed. Consequently, the amount of exergy destroyed in the whole system increases with rising compressor speed. For $T_{\text{cond,ai}} = T_{\text{evap,ai}} = 25^\circ\text{C}$, the AAC system with the VCC for R1234yf and R134a destroyed on average 47.5% and 40.3% less total exergy destruction per unit cooling capacity compared to the system with the FCC, respectively. For the case of $T_{\text{cond,ai}} = T_{\text{evap,ai}} = 40^\circ\text{C}$, the AAC with the VCC for R1234yf and R134a resulted in an average of 18.2% and 26.8% less total exergy destructions per unit cooling capacity compared to the system with the FCC, respectively.

7. Conclusions

This study experimentally investigated the effects of using R1234yf and R134a on the performance of the AAC system for VCC and FCC. Performance comparisons were made for transient and steady-state conditions at different compressor speeds, evaporator and condenser air inlet temperatures and air speeds passing over them. The experimental system was developed from original AAC components in the laboratory environment and equipped with various control and measurement systems to provide data for the performance evaluation. The main results reached in this study are listed below.

- At the compressor speed of 750 rpm, the steady-state value of air temperature leaving the evaporator was 18.60 °C and 18.22 °C for R134a and R1234yf, respectively, when the VCC was employed.
- The mass flow rates of R1234yf and R134a increased by 13.5% and 7.7%, respectively, when the speed of the VCC was increased from 750 rpm to 2750 rpm for $T_{\text{cond,ai}} = T_{\text{evap,ai}} = 40^\circ\text{C}$. For the same air inlet temperatures, the mass flow rates of R1234yf and R134a increased by 54.6% and 66.3%, respectively, when the speed of the FCC compressor was increased from 750 rpm to 2750 rpm.
- In the AAC system with the VCC, the cooling capacities of the system with R1234yf and R134a were in the range of 1.11–3.80 kW and 2.07–3.11 kW, respectively. In the AAC system with the FCC, the cooling capacities for R1234yf and R134a were in the range of 2.86–4.39 kW and 2.88–4.63 kW, respectively.
- For $T_{\text{cond,ai}} = T_{\text{evap,ai}} = 40^\circ\text{C}$, the AAC system with R1234yf using VCC and FCC had on average 13.6% and 20.1% less COP than the system with R134a using the same compressors, respectively. For $T_{\text{cond,ai}} = T_{\text{evap,ai}} = 25^\circ\text{C}$, the COP for the R1234yf system was on average 1.1% higher than the COP for the R134a one, the capacity control system of the VCC system is more effective in the system with R1234yf than that with R134a at high compressor speeds.
- The AAC system using R1234yf with VCC and FCC has lower compressor discharge temperatures 1.87–7.51 °C and 3.44–12.03 °C, respectively, than the system with R134a for the same compressor types.
- The amount of exergy destroyed in the AAC components of the system with the VCC was found to be between 1.7% and 52.7% compared to the system with the FCC.
- In the AAC system with R1234yf refrigerant, the amount of exergy destroyed in the evaporator and condenser components is lower than

in the system with R134a, and the exergy destroyed in the compressor and TXV is higher.

- The total amount of exergy destroyed per unit cooling capacity in the AAC system with the VCC was found to be 18.2% – 47.5% lower than that of the FCC.

Comparing the performance parameters of the R1234yf AAC system for the VCC with the literature, the COP obtained in this study is 6.3% higher than that found in Alkan et al. (2021) and 2.1% higher than that in Cho and Park (2016). Considering the results of this study, the use of R1234yf with VCC seems to be the best alternative to R134a and more environmentally friendly despite the decrease in some performance parameters. In future studies, the effect of using IHX on the performance of an R1234yf AAC system with a VCC can be investigated. Furthermore, the influence of other R134a alternatives such as R1234ze(E) on the performance of an AAC system with the VCC can be investigated.

Declaration of Competing Interest

The authors declare that they have no known competing financial interests or personal relationships that could have appeared to influence the work reported in this paper.

Acknowledgments

This study was supported by the Research Fund of the Sakarya University of Applied Science Project Number: 2020-50-01-002. All authors would like to thank the individuals who were involved in making this work possible.

References

- Alkan, A., Hosoz, M., 2010a. Comparative performance of an automotive air conditioning system using fixed and variable capacity compressors. *Int. J. Refrig.* 33, 487–495. <https://doi.org/10.1016/j.ijrefrig.2009.12.018>.
- Alkan, A., Hosoz, M., 2010b. Experimental performance of an automobile air conditioning system using a variable capacity compressor for two different types of expansion devices. *Int. J. Vehicle Design* 52, 160–176. <https://doi.org/10.1504/ijvd.2010.029642>.
- Alkan, A., Kolp, A., Hosoz, M., 2021. Energetic and exergetic performance comparison of an experimental automotive air conditioning system using refrigerants R1234yf and R134a. *J. Therm. Eng.* 7, 1163–1173. <https://doi.org/10.18186/thermal.978014>.
- Aral, M.C., Suhermanto, M., Hosoz, M., 2021. Performance evaluation of an automotive air conditioning and heat pump system using R1234yf and R134a. *Sci. Technol. Built Environ.* 27, 44–60. <https://doi.org/10.1080/23744731.2020.1776067>.
- Cattelan, G., Diani, A., Azzolin, M., 2022. Condensation heat transfer of R1234ze (E) and R134a inside a brazed plate heat exchanger: Experimental data and model assessment. *J. Int. Refrig.* 143, 57–67. <https://doi.org/10.1016/j.ijrefrig.2022.06.022>.
- Cho, H., Lee, H., Park, C., 2013. Performance characteristics of an automobile air conditioning system with internal heat exchanger using refrigerant R1234yf. *Appl. Therm. Eng.* 61, 563–569. <https://doi.org/10.1016/j.applthermaleng.2013.08.030>.
- Cho, H., Park, C., 2016. Experimental investigation of performance and exergy analysis of automotive air conditioning systems using refrigerant R1234yf at various compressor speeds. *Appl. Therm. Eng.* 101, 30–37. <https://doi.org/10.1016/j.applthermaleng.2016.01.153>.
- Daly, S., 2006. Automotive air conditioning and climate control systems. Butterworth-Heinemann. <https://doi.org/10.1016/B978-0-7506-6955-9.X5000-9>.
- Daviran, S., Kasaean, A., Golzari, S., Mahian, O., Nasirivatan, S., Wongwises, S., 2017. A comparative study on the performance of HFO-1234yf and HFC-134a as an alternative in automotive air conditioning systems. *Appl. Therm. Eng.* 110, 1091–1100. <https://doi.org/10.1016/j.applthermaleng.2016.09.034>.
- Devecioğlu, A., Oruç, V., 2018. Improvement on the energy performance of a refrigeration system adapting a plate-type heat exchanger and low-GWP refrigerants as alternatives to R134a. *Energy* 155, 105–116. <https://doi.org/10.1016/j.energy.2018.05.032>.
- Gaurav, Kumar, R., 2018. Computational energy and exergy analysis of R134a, R1234yf, R1234ze and their mixtures in vapour compression system. *Ain Shams Eng. J.* 9 (4), 3229–3237. <https://doi.org/10.1016/j.asej.2018.01.002>.
- Global Environmental Change Report GCRP, 1997. A brief analysis Kyoto protocol, vol. IX, p. 24.
- Golzari, S., Kasaean, A., Daviran, S., Mahian, O., Wongwises, S., Sahin, A.Z., 2017. Second law analysis of an automotive air conditioning system using HFO-1234yf, an environmentally friendly refrigerant. *Int. J. Refrig.* 73, 134–143. <https://doi.org/10.1016/j.ijrefrig.2016.09.009>.
- Hosoz, M., Direk, M., Yigit, K.S., Canakci, M., Turkcan, A., Alptekin, E., Sanli, A., 2015. Performance evaluation of an R134a automotive heat pump system for various heat sources in comparison with baseline heating system. *Appl. Therm. Eng.* 78, 419–427. <https://doi.org/10.1016/j.applthermaleng.2014.12.072>.
- Inan, M.S., 2021. Experimental Investigation of the Effect of Different Circuit Components on the Performance of an Automobile Air Conditioning System Using R134a and R1234yf. MSc Thesis. Sakarya University of Applied Sciences, Sakarya, Turkey, (in Turkish).
- Khatoun, S., Karimi, M., 2023. Thermodynamic analysis of two evaporator vapor compression refrigeration system with low GWP refrigerants in automobiles. *Int. J. Air-Cond. Ref.* 31, 2. <https://doi.org/10.1007/s44189-022-00017-1>.
- Kumar, V., Karimi, M.N., Kamboj, S.K., 2020. Comparative analysis of cascade refrigeration system based on energy and exergy using different refrigerant pairs. *J. Therm. Eng.* 6, 106–116. <https://doi.org/10.18186/thermal.671652>.
- Lee, Y., Jung, D., 2012. A brief performance comparison of R1234yf and R134a in a bench tester for automobile applications. *Appl. Therm. Eng.* 35, 240–242. <https://doi.org/10.1016/j.applthermaleng.2011.09.004>.
- Lemmon, E.W., Bell, I.H., Huber, M.L., McLinden, M.O., 2018. NIST Standard Reference Database 23: Reference Fluid Thermodynamic and Transport Properties-REF-PROP, Version 10.0. National Institute of Standards and Technology. Standard Reference Data Program, Gaithersburg.
- Li, Zhaohua, Liang, Kun, Chen, Xinwen, Zhu, Zhennan, Zhu, Zhongpan, Jiang, Hanyang, 2022. A comprehensive numerical model of a vapour compression refrigeration system equipped with a variable displacement compressor. *Appl. Therm. Eng.* 204, 117967. <https://doi.org/10.1016/j.applthermaleng.2021.117967>.
- Mendoza-Miranda, J.M., Mota-Babiloni, A., Ramirez-Minguela, J.J., Muñoz-Carpio, V. D., Carrera-Rodríguez, M., Navarro-Esbrí, J., Salazar-Hernandez, C., 2016. Comparative evaluation of R1234yf, R1234ze (E) and R450A as alternatives to R134a in a variable speed reciprocating compressor. *Energy* 114, 753–766. <https://doi.org/10.1016/j.energy.2016.08.050>.
- Moffat, R.J., 1988. Describing the uncertainties in experimental results. *Exp. Therm. Fluid Sci.* 1, 3–17. [https://doi.org/10.1016/0894-1777\(88\)90043-X](https://doi.org/10.1016/0894-1777(88)90043-X).
- Mota-Babiloni, A., Navarro-Esbrí, J., Barragán, Á., Molés, F., Peris, B., 2014. Drop-in energy performance evaluation of R1234yf and R1234ze(E) in a vapor compression system as R134a replacements. *Appl. Therm. Eng.* 71, 259–265. <https://doi.org/10.1016/j.applthermaleng.2014.06.056>.
- Navarro, E., Martinez-Galvan, I.O., Nohales, J., Gonzalez-Macia, J., 2013. Comparative experimental study of an open piston compressor working with R1234yf, R134a and R290. *Int. J. Refrig.* 36, 768–775. <https://doi.org/10.1016/j.ijrefrig.2012.11.01>.
- Navarro-Esbrí, J., Mendoza-Miranda, J.M., Mota-Babiloni, A., Barragán-Cervera, A., Belman-Flores, J.M., 2013. Experimental analysis of R1234yf as a drop-in replacement for R134a in a vapor compression system. *Int. J. Refrig.* 36, 870–880. <https://doi.org/10.1016/j.ijrefrig.2012.12.01>.
- Ozgener, O., Hepbasli, A., 2007. Modeling and performance evaluation of ground source (geothermal) heat pump systems. *Energy Build.* 39 (1), 66–75. <https://doi.org/10.1016/j.enbuild.2006.04.019>.
- Tasdemirci, E., Alptekin, E., Hosoz, M., 2022. Experimental performance comparison of R1234yf and R134a automobile air conditioning systems employing a variable capacity compressor. *Int. J. Vehicle Design* 90, 1–18. <https://doi.org/10.1504/IJVD.2022.129169>.
- UNEP, 1987. Montreal Protocol on Substances that Deplete the Ozone Layer. Final Act. United Nations, New York.
- Wantha, C., 2019. Analysis of heat transfer characteristics of tube-in-tube internal heat exchangers for HFO-1234yf and HFC-134a refrigeration systems. *Appl. Therm. Eng.* 157, 113747. <https://doi.org/10.1016/j.applthermaleng.2019.113747>.
- Yataganbaba, A., Kilicarslan, A., Kurtba, S., I., 2015. Exergy analysis of R1234yf and R1234ze as R134a replacements in a two evaporator vapour compression refrigeration system. *Int. J. Refrig.* 60, 26–37. <https://doi.org/10.1016/j.ijrefrig.2015.08.010>.
- Zilio, C., Brown, J.S., Schiochet, G., Cavallini, A., 2011. The refrigerant R1234yf in air conditioning systems. *Energy* 36, 6110–6120. <https://doi.org/10.1016/j.energy.2011.08.002>.